On the Use of FDTD and Ray-Tracing Schemes in the Nanonetwork Environment

Journal:	*IEEE Communications Letters*
Manuscript ID:	CL2014-0701
Manuscript Type:	Original Article
Key Words:	Nanotechnology, FDTD methods, Ray tracing, Networks, Simulation
EDICS:	CL1.2.2 Wireless Networks < CL1.2 Wireless Communications, CL1.2 Wireless Communications, CL1.7.3 Performance Analysis < CL1.7 Network Architecture and Design, CL1.8.5 Protocols for Mobile Networks < CL1.8 Communication Protocols

On the Use of FDTD and Ray-Tracing Schemes in the Nanonetwork Environment

Author 1, Author 2, Author 3, Author 4, Author 5, Author 6, and Author 7

***Abstract*—In this letter, the finite difference time-domain (FDTD) method and the ray-tracing (RT) technique are systematically revisited and compared as potential tools that can reliably characterize new protocols for emerging nanonetwork applications. To this aim, a set of efficient simulation schemes for the precise prediction of the reception quality in various communication scenarios is presented. In particular, each algorithm involves a similar configuration with a realistic transmitter/receiver model and multiple obstacles sized up to some micrometers. The proposed analysis reveals that, unlike conventional assessments, the RT approach can rapidly and successfully determine the reception quality at nanoscale dimensions, since its results are in satisfactory agreement with the respective FDTD data. These significant deductions are, finally, substantiated by a theoretical formulation equivalent to that of frequency selective surfaces.**

***Index Terms*—Nanonetwork communications, reception quality, FDTD method, ray-tracing schemes, numerical techniques.**

I. Introduction

SINCE its initial advent, nanotechnology has offered many inspiring and rapidly evolving prospects for almost every scientific discipline and, therefore, human life. Among them, wireless nanonetworks constitute the cutting-edge in the quest for optimal energy, complexity, and cost communication systems [1]–[4]. Nonetheless, the constant requisite for additional size reduction (in the order of few micrometers) and extended connectivity has triggered an intensive protocol research [5]–[7], while new carbon forms have enabled the design of miniaturized antennas at the far infrared spectrum [8]. For the study of these laborious arrangements, explicit numerical methods like the finite-difference time-domain (FDTD) one [9], can be proven markedly instructive, provided that their computational overhead is reasonable. Conversely, ray-tracing-based (RT) algorithms [10], [11] are cheaper to implement, yet they are deemed trustworthy only if the dimensions of all objects in the domain are extensively larger than the examined frequency wavelength. So, in the 0.1-10 THz band, RT techniques are not known whether they are able to perform adequately well.

Motivated by the absence of relevant studies, this letter investigates the applicability of the FDTD and RT method to the analysis of modern nanoscale networks, as versatile tools for the consistent and accurate estimation of their reception quality. To this goal, different setups are developed in terms of robust transmitter/receiver models with diverse micrometer-sized obstacles to compare the performance of both techniques. A key advantage of the novel approach is that it clearly proves the applicability of the RT algorithm in nanoscale dimensions, despite the customary belief, as a trustworthy tool for fast and precise reception quality predictions, even in the demanding case of multiple obstacles. In fact, the RT scheme responds remarkably well and in very good accordance with the FDTD results. These interesting findings are properly justified via a theoretical framework based on frequency selective surfaces.

II. Theoretical Analysis and Model Development

The primary strength of the FDTD technique stems from an elegant discretization process for the explicit treatment of wave propagation. Starting from Maxwell's equations, the algorithm establishes a well-posed field assignment on dual grids, staggered in space and time, where second-order central-difference approximants are applied to the differential curl operators of Ampère's and Faraday's laws [9]. So, the method attains a serious sampled-data decrease of continuous electric and magnetic components, spatially and temporally interleaved for the natural fulfillment of boundary conditions. Concerning its overhead, the method fits to the category of "resonance region" schemes, whose characteristic domain dimensions are in the same magnitude order as the wavelength. Actually, the FDTD computational cost increases roughly with the fourth power of mesh resolution, chiefly specified by the simulated space. Hence, the choice of space/time increments must always be in a careful compromise with the geometry of the problem.

Alternatively, if the wavelength is exceedingly small (and not comparable) with regard to the smallest obstacle's size (for values of several μm or beyond), ray-based techniques can offer more efficient simulations in terms of CPU and memory burden. Indeed, compared to exact solvers, RT schemes have much lower system requirements, no complexity-to-frequency dependence, and an easy parallelization, at the expense of a mild trade-off in the overall accuracy. These features are attributed to the theoretical formulation of the method in terms of the geometric theory of optics (GO) and the so-called "high-frequency approximation" [10], according to which high frequency waves may be rigorously described by a discrete number of rays, emanating from the source [11]. Furthermore, Fermat's and energy conservation principles are fulfilled, considering reflection and refraction as in regular ray optics.

Based on these notions, we develop three simulation setups that will certify the potential of the RT and FDTD method to

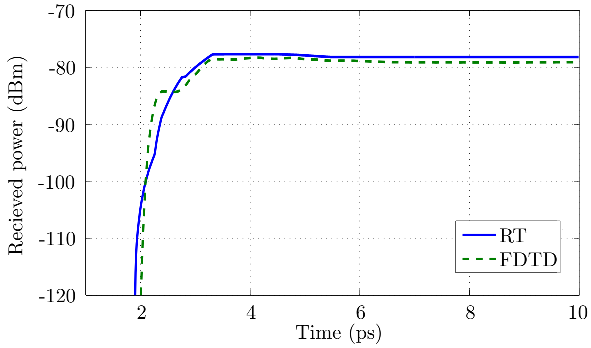

Fig. 1. Energy profile of the FDTD and the RT method at the frequency of 10 THz in the presence of obstacles.

reliably calculate reception quality, even when many nanoscale objects with various intermediate distances are involved.

A. Absence of Obstacles

In the case of an environment without obstacles, there is a line-of-sight connection between the transmitter and the receiver; hence one can anticipate the same amount of energy at the receiver side regardless the method that is employed. Possible discrepancies may appear owing to the FDTD discretization process, the number of initial rays and their spacing from the RT simulation setup as well as the far-field approximation of the latter technique. However, when a finer FDTD cell is selected and the initial arrays are increased and become denser, the two approaches converge to the same results, thus suppressing any artificialities caused by the calculations.

B. Presence of Multiple Obstacles

When several obstacles are included in the simulation scenario, the inevitable scattering of electromagnetic waves from the transmitter (due to their presence) modifies the direction of RT rays. As frequency rises, the RT method can not, theoretically, cope with these reflections, contrary to the FDTD technique. Therefore, the size of local scatterers as compared to the operational wavelength is crucial and alters the behavior of the RT algorithm, leading to deviations in the estimation of signal reception quality between the two approaches.

It is stressed that the "reception quality" term refers to the received time-varying energy level, while both algorithms compute the same energy level but at a slight time offset. The sum of these calculations create the reception quality profile, as in the plot of Fig. 1 at 10 THz. For our analysis, the present work considers a transmitter (antenna), a receiver, and several obstacles of the same size ($\sim 30\,\mu$m). At lower frequencies, such as 2 THz, the wavelength is $150\,\mu$m, namely 5 times larger than the size of the objects in the domain. This issue enforces the RT scheme to estimate higher energy levels, as rays will not be adequately affected by the obstacles. Nevertheless, if frequency increases, the wavelength approaches the value of $29\,\mu$m, which is in the same order of magnitude as the objects' dimensions. Evidently, due to the more prominent multi-directional wave scattering, a larger number of rays will not reach the receiver and thus not taken into account by the RT method, unlike the FDTD one which considers diffraction

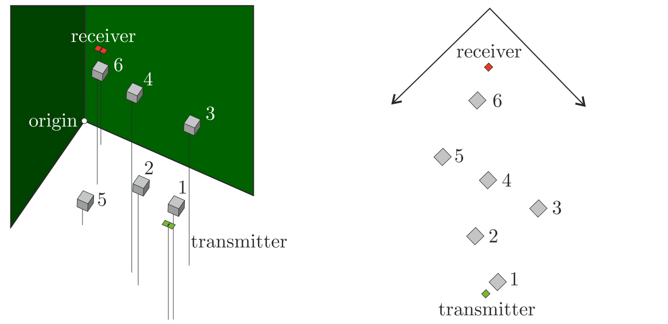

(a) (b)

Fig. 2. (a) Perspective and (b) transverse view of the simulation set up with a receiver (red mark), a transmitter (green mark), and six obstacles (grey cubes). The respective coordinates (in μm) are: receiver $(100, 100, 500)$, transmitter $(500, 500, 500)$, obstacle 1 $(460, 500, 540)$, obstacle 2 $(420, 380, 500)$, obstacle 3 $(260, 440, 600)$, obstacle 4 $(300, 300, 700)$, obstacle 5 $(340, 180, 200)$, and obstacle 6 $(180, 140, 540)$. The origin of the coordinate system is located at the lowest intersection point of the two walls.

phenomena and yields gradually different reception quality results. As the amount of obstacles augments, such divergences are expected to deteriorate because of the extra scattering interactions. From these observations, it becomes apparent why the RT algorithm is commonly presumed inapplicable in the subwavelength regime, as an upshot of its GO approximations.

C. Performance Enhancements via a Diffraction Setup

To improve the accuracy of the RT method, an efficient diffraction computation process is employed in our analysis for the multiple obstacle arrangement. According to the proposed concept, for every ray, the effect of diffracting edges is thoroughly calculated. It is well-known that in the geometric theory of diffraction (GTD), diffraction occurs at points where the field becomes discontinuous. Also, the uniform theory of diffraction (UTD) constitutes the basis for diffraction modeling in many ray-tracing realizations [12]. The latter technique can accurately predict diffracted fields from abrupt material discontinuities for perfectly electric conducting (PEC) obstacles. Initially, first-order diffracting edges are found by searching for adjacent rays which follow different paths through the obstacle (as for discontinuity identification in the GO) and then a diffracting edge can be safely located amid these rays. Thus, by calculating the extra energy attributed to diffraction, the RT formulation is definitely improved in systems with dimensions comparable to the wavelength (e.g. nanonetworks) and attains a sufficiently better agreement with the FDTD results.

III. Numerical Simulations and Results

A. Configuration and Implementation Aspects

The efficiency and applicability comparison of the FDTD and RT methods is conducted by means of the same 3-D simulation environment at the nanoscale level. For this purpose, a lifelike scenario utilizing a couple of nanoantennas, one for transmission and the other for reception, is introduced. These devices are placed inside a $1\,\text{mm}^3$ space formed by two vertically intersecting PEC walls, as shown in Fig. 2. Specifically, the receiver is placed near and the transmitter

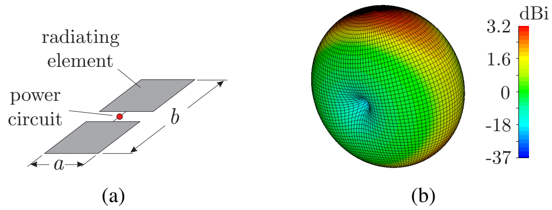

Fig. 3. The transmitting/receiving PEC patch nanoantenna. (a) Geometry with $a = 15\,\mu$m, $b = 60\,\mu$m and (b) radiation pattern.

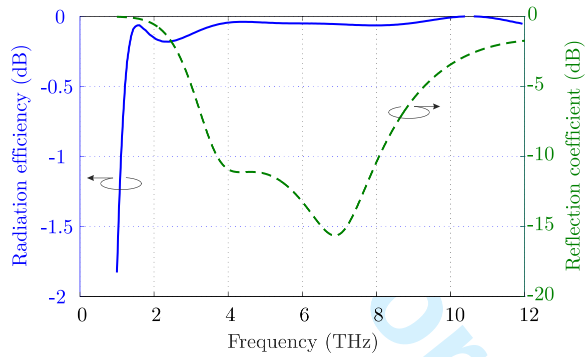

Fig. 4. Radiation efficiency (blue continuous line) and reflection coefficient (green dashed line) of the PEC patch nanoantenna.

adequately far from the 90° corner of the domain, so constructed; both at an equal distance from the walls and the same height in an attempt to achieve a reliable measurement of the propagating electromagnetic energy. Each nanoantenna is considered as a simple $15\,\mu\text{m}\times 60\,\mu\text{m}$ patch (Fig. 3(a)), of two PEC radiating elements and a power circuit, with the pattern of Fig. 3(b) at 6 THz. Also, Fig. 4 shows that the selected device can satisfactorily operate above 2 THz, preserving its reflection coefficient at low levels, until about 10 THz, with the transmitting power set to $1\,\mu$W. For our configuration to be complete, six extra passive nanostructures are interspersed in the domain of Fig. 2 (see caption for their exact coordinates) as real-world obstacles in the receiver's line of sight to thoroughly investigate their impact on the received energy.

Having developed our 3-D computational model, we next proceed to the implementation details of the aforementioned numerical techniques. Hence regarding the FDTD algorithm, the domain is discretized into a lattice of $502 \times 562 \times 360$ cells, which is terminated by 4-cell thick perfectly matched layer absorbing boundary condition [9]. Moreover, the time-update of electric and magnetic field components is performed with a temporal increment of 7.45×10^{-16} sec, whereas the total simulation lasts for 13.42×10^3 time-steps. On the other hand, the RT approach uses a number of 6 reflections, 4 transmissions, and 1 (whenever required) diffraction, for a 0.2° angular ray spacing and a path loss threshold of 70 dB. Finally, both methods involve the normalized input-voltage excitation of Fig. 5 at 6 THz, while our analysis focuses on the spectrum from 2 to 10 THz in order to take into account the theoretical transmission range of modern nanoantennas or nanotubes.

B. Numerical Verification

Our primary objective is to reveal the competence of the RT technique to estimate the reception quality in the nanonetwork

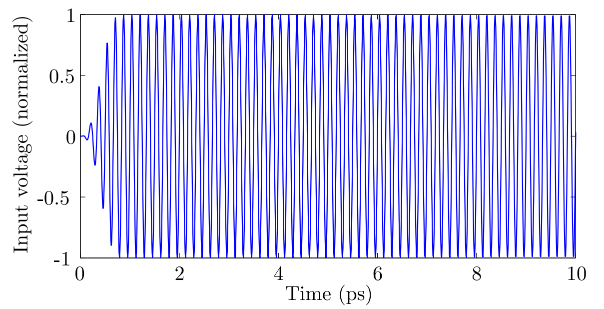

Fig. 5. The normalized input-voltage excitation at the frequency of 6 THz.

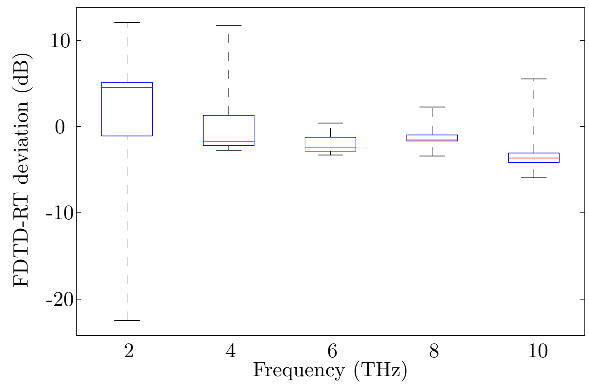

Fig. 6. FDTD-RT deviation for a nanoscale setup in the absence of obstacles. The blue-lined rectangle includes the 50% of all computed simulation results and the red horizontal line depicts their mean value.

environment (herein, in the role of a receiver nanoantenna) as well as to justify its discrepancies with the FDTD method. Let us, first, assume a simulation scenario without any obstacles and compute the received energy in the range of 2 to 10 THz. Figure 6 gives the difference of the two methods in the computation of this energy, where the maximum and minimum deviation occurs at the highest and lowest terminating point of the dashed lines, respectively. Also, the 50% of all (calculated) results is enclosed in the blue-lined rectangle, while their mean value is indicated with a red horizontal line. Obviously, when the rectangle shrinks around the level of 0 dB, the two approaches tend to coincide. Focusing on level of 2 THz in Fig. 6, the mean value deviation of around 5 dB is attributed to the far-field approximation of the RT algorithm. In contrast, at frequencies higher than 4 THz, the aforesaid discrepancy is significantly decreased (less than 2 dB as derived from the 50% rectangles) and simulation outcomes are in excellent agreement. This observation is in complete accordance with the theoretically anticipated estimation, since the line-of-sight is gradually improving, the impact of the diffracted energy from the walls of the setup diminishes, and the RT far-field approximation can be more accurately implemented.

However, when multiple obstacles are present, results, such as in Fig. 7, are found to be positively unexpected, unlike the common belief. Indeed, as frequency increases, one would presume (due to increased ray scattering from the obstacles) that the accuracy of the RT method would deteriorate, concerning the reception relay and received energy from the transmitting nanoantena. Therefore, since at these frequencies the wavelength is comparable to the obstacles's size, the RT technique would have miscalculated the energy of the receiver,

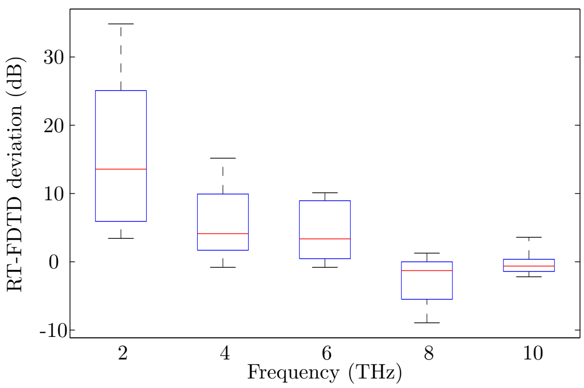

Fig. 7. FDTD-RT deviation for a nanoscale setup in the presence of obstacles. A gradually improving agreement is observed as frequency augments.

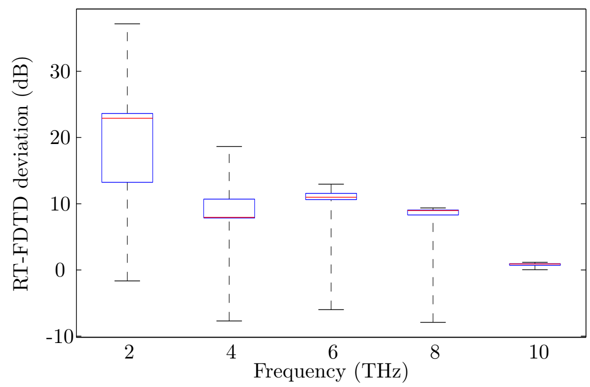

Fig. 8. FDTD-RT deviation in the presence of obstacles and the RT method realized via new diffraction coefficients. The 50% of the calculated values beyond 4 THz for both techniques lies in an interval of less than 3 dB.

owing to its GO conventions, yielding higher values than the real ones. Despite the prior considerations, Fig. 7 presents a very good agreement between the FDTD and the RT schemes, which is constantly improving as frequency increases. Hence it is interesting to mention that the mean value deviation varies below 3 dB between 4 THz and 6 THz, whereas beyond 8 THz these differences become negligible (lower than 0.15 dB).

Evidently, the preceding deductions prove that the RT method can be an instructive means, able to offer reception quality predictions equivalent to the FDTD ones at higher frequencies and nanoscale dimensions. To clarify this behavior, the mesh reflector theory is utilized; so in our simulation models, the group of all dispersed obstacles acts like a capacitive mesh filter, i.e. a frequency selective surface (FSS) [13]. Since such a group is not a 2-D planar mesh and recalling that, at higher frequencies, its size does not seriously influence wave propagation, we consider a surface defined by the vertical projection of every obstacle facing the transmitter. This projection, due to its FSS-based function, offers larger permittivity values, hence explaining the noticeably growing convergence of RT results to their FDTD counterparts with respect to frequency. On the contrary, at lower frequencies, a significant amount of energy is reflected and does not reach the end of the communication channel. Nevertheless, since RT rays are not affected by the setup, the energy at the receiver is artificially increased and, unlike theoretical predictions, the RT method becomes inaccurate, as in the 2 THz case of Fig. 7.

Finally to enhance the RT performance, new diffraction coefficients are computed by extending the analysis of [14] from its original low-frequency (900 MHz) formulation to the nanoscale regime. To this goal, Fig. 8 verifies the technique's advanced precision in the range of 2-10 THz, with a mild trade-off in simulation time. In fact, compared to Fig. 7, the deviation for the 50% of the FDTD and RT values above 4 THz is smaller than 3 dB. Thus, the RT technique can detect even the smaller amount of energy from the diffracting rays, a fact that justifies its improved coincidence with the FDTD data.

IV. Conclusions

The accurate evaluation of reception quality in contemporary nanonetworks via the FDTD and RT technique has been introduced in this letter. To this aim, three scenarios have been devised, namely a line-of-sight one, a configuration with multiple objects dispersed near the line-of-sight, and an obstacle-based RT diffraction setup. Our study unveiled that, despite the traditional aspect, RT results are evenly precise as the FDTD data at the THz spectrum, even in the case of many objects or without considering the diffraction. However, the latter seriously improves the RT accuracy, with a minor time increase. Such deductions reinstate the use of RT schemes as reliable reception quality evaluators in nanoscale dimensions, where networks comprise excessive numbers of nodes.

References

[1] R. Oliveira, M. Luis, L. Bernardo, and R. Dinis, "Towards reliable broadcast in ad hoc networks," *IEEE Commun. Lett.*, vol. 16, no. 3, pp. 1089–1092, 2012.

[2] W. Mo, J. He, M. Karbassian, and J. Wissinger, "Quality of transmission awareness in converged electronic and optical networks with OpenFlow," *IEEE Commun. Lett.*, vol. 17, no. 5, pp. 1036–1039, 2013.

[3] S. Luryi, J. Xu, and A. Zaslavsky, *Future Trends in Microelectronics: Frontiers and Innovations*. Hoboken, NJ: Wiley-IEEE Press, 2013.

[4] *Nano Commun. Networks, Special Issue on Fundamentals of Nanoscale Communications*, vol. 1, no. 3, 2010.

[5] P. A. Martin, P. J. Smith, , and R. Munch, "Improving space-time code performance in slow fading channels using reconfigurable antennas," *IEEE Commun. Lett.*, vol. 16, no. 4, pp. 494–497, 2012.

[6] S. Paris and C. A., "Correlation of wireless link quality: A distributed approach for computing the reception correlation," *IEEE Commun. Lett.*, vol. 16, no. 12, pp. 1341–1343, 2012.

[7] T. Fath and H. Haas, "Performance comparison of MIMO techniques for optical wireless communications in indoor environments," *IEEE Trans. Commun.*, vol. 61, no. 2, pp. 733–742, 2013.

[8] I. Llatser, C. Kremers, A. Cabellos-Aparicio, J. M. Jornet, E. Alarcón, and D. N. Chigrin, "Graphene-based nano-patch antenna for terahertz radiation," *Photonics and Nanostructures — Fundamentals and Applications*, vol. 10, no. 4, pp. 353–358, 2012.

[9] A. Taflove and S. Hagness, *Computational Electrodynamics: The Finite-Difference Time-Domain Method*. Boston, MA: Artech House, 2005.

[10] Z. Zhang, R. Sorensen, Z. Yun, M. Iskander, and J. Harvey, "A ray-tracing approach for indoor/outdoor propagation via window structures," *IEEE Trans. Antennas Propag.*, vol. 50, no. 5, pp. 742–749, 2002.

[11] M. Salem, M. Ismail, and N. Misran, "Validation of three-dimensional ray-tracing algorithm for indoor wireless propagations," *ISRN Commun. Networking*, vol. 2011, pp. 1–5, 2011.

[12] H.-F. Harms, "Using wire grid structures in the combination of uniform geometric theory of diffraction and method of moments for near-field analysis," *Radio Sci.*, vol. 35, no. 2, pp. 639–652, 2000.

[13] J. Zhang, J.-Y. Ou, N. Papasimakis, Y. Chen, K. F. MacDonald, and N. I. Zheludev, "Continuous metal plasmonic frequency selective surfaces," *Opt. Express*, vol. 19, no. 23, p. 23279, 2011.

[14] K. Remley, H. Anderson, and A. Weisshar, "Improving the accuracy of ray-tracing techniques for indoor propagation modeling," *IEEE Trans. Vehicular Technol.*, vol. 49, no. 6, pp. 2350–2358, 2000.